

# Structure–activity relationships in the inhibition of monoamine oxidase B by 1-methyl-3-phenylpyrroles

Modupe O. Ogunrombi,<sup>a</sup> Sarel F. Malan,<sup>a</sup> Gisella Terre'Blanche,<sup>a</sup>  
Neal Castagnoli, Jr.,<sup>b</sup> Jacobus J. Bergh<sup>a</sup> and Jacobus P. Petzer<sup>a,\*</sup>

<sup>a</sup>Pharmaceutical Chemistry, School of Pharmacy, North-West University, Private Bag X6001, Potchefstroom 2520, South Africa

<sup>b</sup>Department of Chemistry, Virginia Tech, Blacksburg, VA 24061, USA

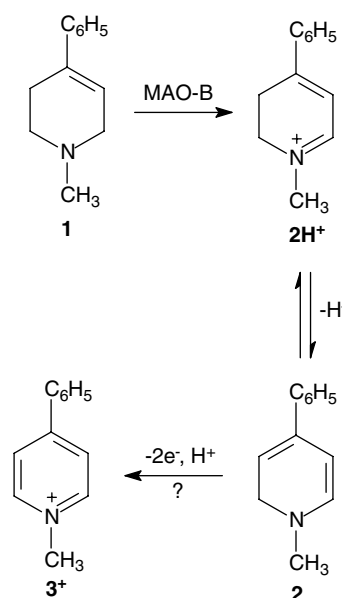
Received 20 July 2007; revised 13 November 2007; accepted 21 November 2007

Available online 28 November 2007

**Abstract**—1-Methyl-3-phenyl-3-pyrrolines are structural analogues of the neurotoxin 1-methyl-4-phenyl-1,2,3,6-tetrahydropyridine (MPTP) and like MPTP are selective substrates of monoamine oxidase B (MAO-B). As part of an ongoing investigation into the substrate properties of various 1-methyl-3-phenyl-3-pyrrolinyl derivatives, it is shown in the present study that their respective MAO-B catalyzed oxidation products act as reversible competitive inhibitors of the enzyme. The most potent inhibitor among the oxidation products considered was 1-methyl-3-(4-trifluoromethylphenyl)pyrrole with an enzyme-inhibitor dissociation constant ( $K_i$  value) of 1.30  $\mu\text{M}$ . The least potent inhibitor was found to be 1-methyl-3-phenylpyrrole with a  $K_i$  value of 118  $\mu\text{M}$ . The results of an SAR study established that the potency of MAO-B inhibition by the 1-methyl-3-phenylpyrrolyl derivatives examined here is dependent on the Taft steric parameter ( $E_s$ ) and Swain–Lupton electronic constant ( $F$ ) of the substituents attached to C-4 of the phenyl ring. Electron-withdrawing substituents with a large degree of steric bulkiness appear to enhance inhibition potency. Potency was also found to vary with the substituents at C-3, again with  $E_s$  and  $F$  being the principal substituent descriptors.  
© 2007 Elsevier Ltd. All rights reserved.

## 1. Introduction

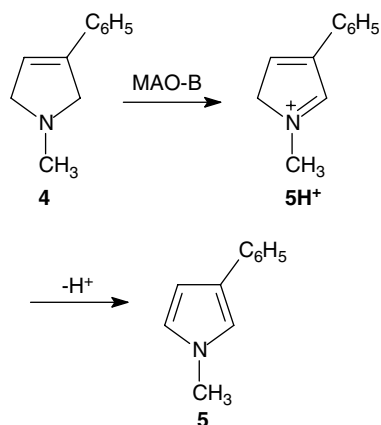
The first step in the metabolic activation of the parkinsonian inducing proneurotoxin, 1-methyl-4-phenyl-1,2,3,6-tetrahydropyridine [MPTP, (**1**)], is catalyzed by the flavoenzyme, monoamine oxidase B (MAO-B) (Scheme 1),<sup>1,2</sup> to yield the ring  $\alpha$ -carbon 2-electron oxidation product, the corresponding 1-methyl-4-phenyl-2,3-dihydropyridinium species MPDP<sup>+</sup> (**2H<sup>+</sup>**). This metabolic intermediate, presumably via the corresponding conjugate base **2**, undergoes a second 2-electron oxidation to generate the 1-methyl-4-phenylpyridinium metabolite MPP<sup>+</sup> (**3<sup>+</sup>**), the ultimate neurotoxin.<sup>3,4</sup> Literature reports various structural analogues of MPTP that have been found to act as good substrates of MAO-B<sup>5,6</sup> as well as of MAO-A.<sup>7</sup> Among these is 1-methyl-3-phenyl-3-pyrroline (**4**) (Scheme 2) which, like MPTP, is a cyclic tertiary allylamine exhibiting selectivity for the MAO-B isoform.<sup>8</sup> The MAO-B catalyzed ring  $\alpha$ -carbon



**Scheme 1.** The MAO-B catalyzed oxidation of MPTP (**1**) to yield the corresponding dihydropyridinium product MPDP<sup>+</sup> (**2H<sup>+</sup>**) which spontaneously undergoes a second 2-electron oxidation to generate MPP<sup>+</sup> (**3<sup>+</sup>**).

**Keywords:** Monoamine oxidase B; Reversible inhibitors; Competitive inhibition; 1-Methyl-3-phenylpyrrole; Structure–activity relationship.

\* Corresponding author. Tel.: +27 18 2992206; fax: +27 18 2994243; e-mail: jacques.petzer@nwu.ac.za



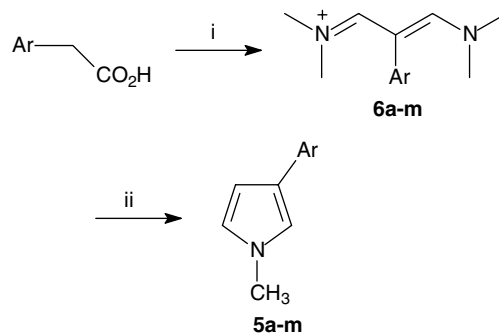
**Scheme 2.** The MAO-B catalyzed oxidation of 1-methyl-3-phenyl-3-pyrrolinyl derivatives (**4**) to yield the corresponding 1-methyl-3-phenylpyrrolyl products (**5**). This oxidation most likely arises via **5H<sup>+</sup>**, the short-lived conjugate acid of the pyrrolyl product **5**.

2-electron oxidation of **4** yields 1-methyl-3-phenylpyrrole (**5**) as the final product. This oxidation most likely arises via **5H<sup>+</sup>**, the short-lived conjugate acid of the pyrrolyl product **5**.<sup>9</sup> As part of an ongoing investigation into the substrate properties of various 1-methyl-3-phenyl-3-pyrrolinyl derivatives, it is shown in the present study that their respective MAO-B catalyzed oxidation products act as reversible competitive inhibitors of the enzyme. A literature survey reveals that reversible inhibition of MAO-B by 1-methyl-3-phenylpyrrole (**5a**) and its 4-chlorophenyl analogue (**5b**) has previously been demonstrated.<sup>10</sup> In an attempt to determine the effect that specific structural modifications of 1-methyl-3-phenylpyrrole will have on MAO-B inhibition potency, we have synthesized 13 1-methyl-3-phenylpyrrolyl derivatives (**5a–m**) and determined their enzyme-inhibitor dissociation constants ( $K_i$  values) for reversible interaction with MAO-B. As part of the present SAR analysis, the 1-methyl-3-phenylpyrrolyl derivatives investigated differed only in the substituents on C-3 and C-4 of the phenyl ring. Since inhibitors of MAO-B are currently in use and being investigated for the treatment of neurodegenerative disorders,<sup>11,12</sup> the results of this study may aid in the identification and design of new reversible inhibitors.

## 2. Results

### 2.1. Chemistry

The 1-methyl-3-phenylpyrrolyl derivatives (**5a–m**) examined in this study were prepared in relatively good yields (26.6–72.7%) according to a previously reported procedure (Scheme 3).<sup>13</sup> The key starting materials were the 2-aryl-3-(dimethylamino)allylidene(dimethyl)ammonium perchlorates (**6a–m**) which were prepared in very high yields from the appropriately substituted phenylacetic acid derivatives and DMF.<sup>14</sup> Cyclization of **6**, to yield the target pyrrolyl derivatives (**5a–m**), was achieved by treatment with sodium methoxide in anhydrous pyridine. Following purification by column chromatography or by recrystallization from a suitable



**Scheme 3.** Synthetic pathway to 1-methyl-3-phenylpyrroles (**5a–m**). Reagents and conditions: (i) DMF, POCl<sub>3</sub>, 80 °C; (ii) NaOCH<sub>3</sub>, pyridine, reflux.

solvent, the structures and purity of the compounds were verified by mass spectrometry, <sup>1</sup>H NMR, and <sup>13</sup>C NMR. For those compounds previously reported, the physical data and melting points obtained were compared to the corresponding literature values as cited in Section 4.

### 2.2. Enzymology and inhibition studies

In the present study we have determined the enzyme-inhibitor dissociation constants ( $K_i$  values) for reversible interaction of MAO-B with members of a synthetic series of 1-methyl-3-phenylpyrrolyl derivatives (**5a–m**). MAO-B activity measurements were based on the ring  $\alpha$ -carbon oxidation of 1-methyl-4-(1-methylpyrrol-2-yl)-1,2,3,6-tetrahydropyridine (MMTP) to yield the corresponding dihydropyridinium species (MMDP<sup>+</sup>).<sup>15</sup> The concentrations of MMDP<sup>+</sup> produced by this enzymatic reaction were measured spectrophotometrically since MMDP<sup>+</sup> absorbs light maximally at 420 nm. At this wavelength neither the enzyme substrate nor the test inhibitors absorb light. Because of these favorable chromophoric characteristics and the in vitro chemical stability of MMDP<sup>+</sup>, this assay is frequently used to evaluate the potencies of potential inhibitors of MAO-B.<sup>16,17</sup> The mitochondrial fraction obtained from baboon liver tissue was employed as enzyme source since it exhibits a high degree of MAO-B catalytic activity and is devoid of MAO-A activity.<sup>15</sup> Therefore, even though MMTP is a MAO-A/B mixed substrate, its oxidation by baboon liver mitochondria can be attributed exclusively to the action of the MAO-B isoform. The interaction of reversible inhibitors with MAO-B obtained from baboon liver tissue appears to be similar to the interaction with the human form of the enzyme since inhibitors are approximately equipotent with both enzyme sources.<sup>17</sup>

The MAO-B inhibitory properties of **5a–m** first were investigated in order to determine whether the test inhibitors act as time-dependent inactivators or reversible inhibitors of the enzyme. For this study **5e** was selected as a representative test inhibitor. When baboon liver mitochondrial fractions were preincubated with **5e** (5.20  $\mu$ M) for periods of 0, 15, 30, and 60 min, the rate of MAO-B catalyzed oxidation of MMTP (90  $\mu$ M) to MMDP<sup>+</sup> remained unchanged (results not shown).<sup>18</sup>

From this result it can be concluded that **5e** interacts reversibly with the active site of MAO-B. The reversibility of enzyme inhibition by **5a–m** was also apparent from the Lineweaver–Burk plots constructed from the kinetic data (see below).

All of the 1-methyl-3-phenylpyrrolyl derivatives (**5a–m**) evaluated were found to be inhibitors of MAO-B. As demonstrated with 1-methyl-3-(3-chlorophenyl)pyrrole (**5h**) (Fig. 1), classical Lineweaver–Burk plots for competitive inhibition were obtained for all of the test inhibitors. The enzyme-inhibitor dissociation constants ( $K_i$  values) for the inhibition of MAO-B by **5a–m** are presented in Table 1. The data lead to the conclusion that substitution on the phenyl ring leads to inhibitors with enhanced inhibition potencies since **5a** was found to be the weakest inhibitor. The most potent inhibitor of the series was 1-methyl-3-(4-trifluoromethylphenyl)pyrrole (**5e**) with a  $K_i$  value of 1.30  $\mu\text{M}$ . The second most potent inhibitor of the series was 1-methyl-3-(3-trifluoromethylphenyl)pyrrole (**5k**) with a  $K_i$  value of 6.55  $\mu\text{M}$ . Substitution at C-4 or C-3 of the phenyl ring with the electronegative  $\text{CF}_3$  functional group therefore appears to be the best method of enhancing the binding affinity of 1-methyl-3-phenylpyrrolyl derivatives for the active site of MAO-B. Interestingly, no inhibition of beef liver MAO-B was observed by **5e**, even at a concentration of 200  $\mu\text{M}$  (results not shown). Similarly, no inhibition of beef liver MAO-B was observed by any of the other pyrrolyl derivatives examined here. Further inspection of Table 1 reveals that substitution with bromine at C-4 (**5c**) and C-3 (**5i**) also results in pyrrolyl derivatives with relatively high inhibition potencies. Since substitution at C-4 (**5d**) and C-3 (**5j**) of the phenyl ring with fluorine resulted in relatively weaker inhibitors compared to the bromine analogues **5c** and **5i** and chlorine analogues

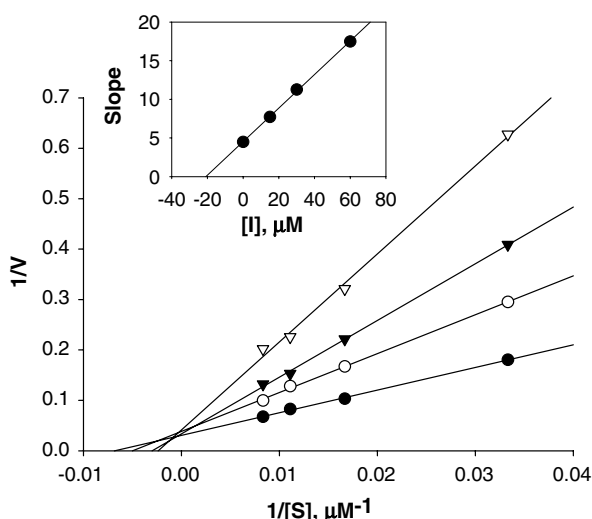
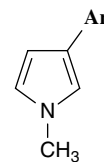


**Figure 1.** Lineweaver–Burk plots of the oxidation of MMTP by baboon liver MAO-B in the absence (filled circles) and presence of various concentrations of **5h** (open circles, 15  $\mu\text{M}$ ; filled triangles, 30  $\mu\text{M}$ ; and open triangles, 60  $\mu\text{M}$ ). The concentration of the baboon liver mitochondrial isolate was 0.15 mg/mL and the rates are expressed as nmol/min mg protein of  $\text{MMDP}^+$  formed. The inset is the replot of the slopes versus the inhibitor concentration.

**Table 1.** The  $K_i$  values for the inhibition of MAO-B by 1-methyl-3-phenylpyrrolyl derivatives (**5a–m**)



Compound	Ar	$K_i$ value ( $\mu\text{M}$ ) <sup>a</sup>	$E_s$ <sup>b</sup>	$F^b$
<b>5a</b>	$\text{C}_6\text{H}_5$	118	0.00	0.00
<b>5b</b>	4- $\text{ClC}_6\text{H}_4$	18.4	-0.97	0.42
<b>5c</b>	4- $\text{BrC}_6\text{H}_4$	6.65	-1.16	0.45
<b>5d</b>	4- $\text{FC}_6\text{H}_4$	31.0	-0.46	0.45
<b>5e</b>	4- $\text{CF}_3\text{C}_6\text{H}_4$	1.30	-2.40	0.38
<b>5f</b>	4- $\text{CH}_3\text{C}_6\text{H}_4$	22.5	-1.24	0.01
<b>5g</b>	4- $\text{OCH}_3\text{C}_6\text{H}_4$	36.5	-0.55	0.29
<b>5h</b>	3- $\text{ClC}_6\text{H}_4$	20.9	-0.97	0.42
<b>5i</b>	3- $\text{BrC}_6\text{H}_4$	14.3	-1.16	0.45
<b>5j</b>	3- $\text{FC}_6\text{H}_4$	38.9	-0.46	0.45
<b>5k</b>	3- $\text{CF}_3\text{C}_6\text{H}_4$	6.55	-2.40	0.38
<b>5l</b>	3- $\text{CH}_3\text{C}_6\text{H}_4$	56.0	-1.24	0.01
<b>5m</b>	3- $\text{OCH}_3\text{C}_6\text{H}_4$	41.7	-0.55	0.29

The values of the selected physicochemical parameters used in the SAR studies are also listed.

<sup>a</sup> The enzyme source used was baboon liver mitochondrial MAO-B.

<sup>b</sup> Values obtained from Ref. 19.

**5b** and **5h**, it does not appear that potent inhibition is linked exclusively to the presence of electronegative substituents in the phenyl ring.

### 2.3. Quantitative structure–activity relationships (QSAR)

In an attempt to quantify the relationship between MAO-B inhibitory activity and the physicochemical properties of the substituents, a Hansch-type SAR study was carried out by multiple linear regression analysis. Five parameters were used to describe each substituent. The Taft steric parameter ( $E_s$ )<sup>19</sup> and the Van der Waals volume ( $V_w$ )<sup>20</sup> were used as descriptors of bulkiness while the lipophilicities of the substituents were described by the Hansch constant ( $\pi$ ).<sup>19</sup> The classical Hammett ( $\sigma_m$  or  $\sigma_p$ ) and Swain–Lupton ( $F$ ) constants served as electronic parameters.<sup>19</sup> All the physicochemical values of the substituents were obtained from standard compilations.<sup>19,20</sup> The analogues were divided into two groups—those bearing substituents at C-4 of the phenyl ring (**5b–g**) and those with substituents at C-3 of the phenyl ring (**5h–m**). The unsubstituted 1-methyl-3-phenylpyrrole (**5a**) was considered a member of both groups. Results of the statistical analysis for the two groups are shown in Tables 2 and 3, respectively.

For analogues substituted at C-4 of the phenyl ring (Table 2), the Taft steric parameter ( $E_s$ ) was the only substituent descriptor that showed a meaningful correlation with the logarithm of the  $K_i$  values (expressed in micromolar). Regression analysis of  $\log K_i$  with  $E_s$  exhibited a relatively good correlation with a  $R^2$  value of 0.91. The statistical  $F$  value for the correlation was found to be 51.7, which is higher than the  $F_{\text{max}}$  value (25.32)<sup>21</sup> for

**Table 2.** Correlations of the MAO-B inhibition constants ( $\log K_i$ ) of the 1-methyl-3-phenylpyrrolyl derivatives (**5a–g**) with steric, electronic, and hydrophobic descriptors of the substituents at C-4 of the phenyl ring<sup>a</sup>

Parameter	Slope	y-Intercept	R <sup>2</sup>	F <sup>b</sup>	Significance <sup>c</sup>
$\sigma_p$	$-1.76 \pm 0.64$	$1.40 \pm 0.17$	0.60	7.54	0.041
$F$	$-1.67 \pm 1.18$	$1.72 \pm 0.40$	0.29	2.00	0.22
$V_w$	$-1.17 \pm 1.05$	$1.01 \pm 0.31$	0.20	1.23	0.32
$\pi$	$-1.30 \pm 0.38$	$1.82 \pm 0.22$	0.70	11.6	0.019
$E_s$	$0.77 \pm 0.11$	$1.99 \pm 0.13$	0.91	51.7	0.0008
$E_s + F$	$0.71 \pm 0.07$	$2.16 \pm 0.09$	0.98	79.7	0.0004
	$-0.83 \pm 0.26$				0.032

<sup>a</sup> The logarithm of the  $K_i$  values expressed in micromolar was used in the linear regression analysis.

<sup>b</sup> Higher  $F$  values indicate a better fit and a regression equation with an  $F$  value higher than the critical  $F$  value may be judged as significant. Critical  $F$  values may be calculated as described recently.<sup>21</sup>

<sup>c</sup> The significance is the fractional probability that the coefficient of the added variable is zero.

**Table 3.** Correlations of the MAO-B inhibition constants ( $\log K_i$ ) of the 1-methyl-3-phenylpyrrolyl derivatives (**5a** and **h–m**) with steric, electronic, and hydrophobic descriptors of the substituents at C-3 of the phenyl ring<sup>a</sup>

Parameter	Slope	y-Intercept	R <sup>2</sup>	F <sup>b</sup>	Significance <sup>c</sup>
$\sigma_m$	$-1.69 \pm 0.49$	$1.86 \pm 0.14$	0.71	12.0	0.018
$F$	$-1.52 \pm 0.63$	$1.91 \pm 0.22$	0.54	5.75	0.062
$V_w$	$-0.47 \pm 0.29$	$1.91 \pm 0.30$	0.34	2.52	0.17
$\pi$	$-0.84 \pm 0.27$	$1.85 \pm 0.16$	0.65	9.34	0.028
$E_s$	$0.46 \pm 0.12$	$1.92 \pm 0.15$	0.73	13.6	0.014
$E_s + F$	$0.38 \pm 0.05$	$2.14 \pm 0.06$	0.97	72.2	0.0013
	$-1.07 \pm 0.18$				0.0039

<sup>a</sup> The logarithm of the  $K_i$  values expressed in micromolar were used in the linear regression analysis.

<sup>b</sup> Higher  $F$  values indicate a better fit and a regression equation with an  $F$  value higher than the critical  $F$  value may be judged as significant. Critical  $F$  values may be calculated as described recently.<sup>21</sup>

<sup>c</sup> The significance is the fractional probability that the coefficient of the added variable is zero.

95% significance (a higher  $F$  value indicates a better fit). All other single-parameter fits with the  $\log K_i$  values exhibited poorer statistical correlations. Correlations could be improved by the inclusion of an additional substituent parameter in the regression analysis. A two-parameter fit with  $E_s$  and the Swain–Lupton constant ( $F$ ) yielded a model with a  $R^2$  value of 0.98 and a statistical  $F$  value of 79.7 ( $F_{\max} = 30.18$ ). For this correlation, the probabilities that  $E_s$  and  $F$  are zero are 0.04% and 3.2%, respectively. Therefore, the best mathematical description of binding affinity ( $\log K_i$ ) of the C-4 substituted 1-methyl-3-phenylpyrroles (**5a–g**) to MAO-B is:

$$\log K_i = 0.71(\pm 0.07)E_s - 0.83(\pm 0.26)F + 2.16(\pm 0.09) \quad (1)$$

$$(R^2 = 0.98 \text{ and } F = 79.7)$$

Since bulky substituents have increasingly negative Taft steric parameter ( $E_s$ ) values, the positive correlation observed with  $E_s$  ( $0.71 \pm 0.07$ ) indicates that the MAO-B inhibition potency ( $\log K_i$ ) may be enhanced by substitution at C-4 of the phenyl ring with a bulky substituent

(Fig. 2). The negative correlation between  $\log K_i$  and  $F$  ( $-0.83 \pm 0.26$ ) indicates that the potency ( $\log K_i$ ) by which 1-methyl-3-phenylpyrroles inhibit MAO-B may be enhanced by substitution with electron-withdrawing C-4 functional groups. Although not statistically significant, there also appears to be a moderate correlation ( $R^2 = 0.70$ ) between inhibitor binding affinity ( $\log K_i$ ) and the lipophilicity ( $\pi$ ) of the C-4 substituents. Since more lipophilic substituents have increasingly positive Hansch constant ( $\pi$ ) values, the negative correlation ( $-1.30 \pm 0.38$ ) between  $\pi$  and the  $\log K_i$  values indicates that enhancement of the lipophilicity of the C-4 substituents may lead to better inhibition potency. The observed linear correlations of  $\log K_i$  with both  $E_s$  and  $\pi$  are to be expected since, for the set of substituents examined here, there exists a moderate correlation ( $R^2 = 0.68$ ) between these two substituent descriptors. No significant correlations were observed for any other combination of two substituent descriptors.

For analogues substituted at C-3 of the phenyl ring (Table 3), there appeared to be no single substituent descriptor that showed a meaningful correlation with

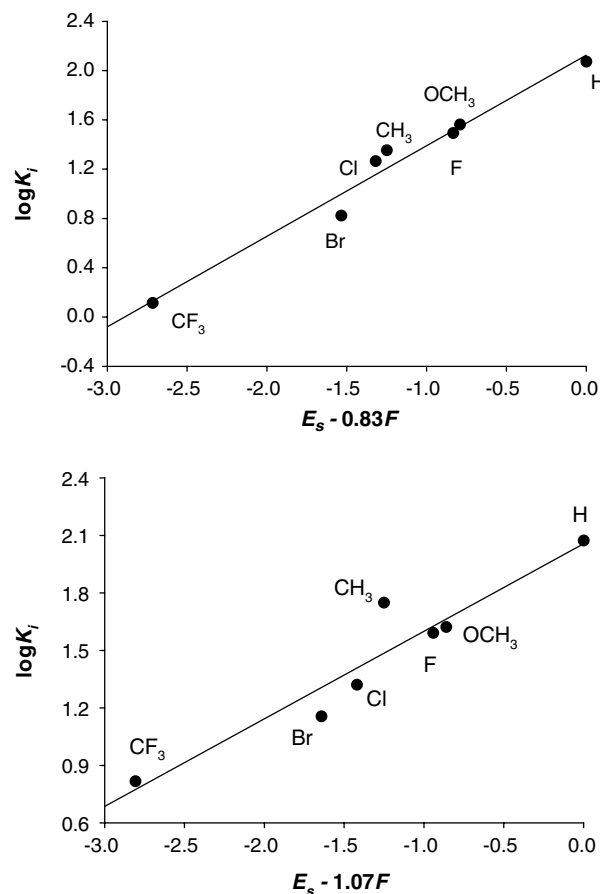


**Figure 2.** Correlations of the  $\log K_i$  values for the inhibition of MAO-B by **5a–m** with the Taft steric parameter ( $E_s$ ) of the substituents at C-4 (top) and C-3 (bottom) of the phenyl ring. The  $E_s$  values were adjusted by the contribution of the Swain–Lupton  $F$  constant as indicated on the x-axis titles. The linear regression lines are graphical representations of Eqs. 1 and 2 and the correlation coefficients are 0.98 and 0.97, respectively.

the  $\log K_i$  values. A two-parameter fit with  $E_s$  and the Swain–Lupton constant ( $F$ ), however, yielded a model with a  $R^2$  value of 0.97 and a statistical  $F$  value of 72.2 ( $F_{\max} = 30.18$ ). For this correlation, the probabilities that  $E_s$  and  $F$  are zero are 0.13% and 0.39%, respectively. Therefore, the best mathematical description of binding affinity ( $\log K_i$ ) of the C-3 substituted 1-methyl-3-phenylpyrroles (**5a** and **h–m**) to MAO-B is:

$$\log K_i = 0.38(\pm 0.05)E_s - 1.07(\pm 0.18)F + 2.14(\pm 0.06)$$

$$(R^2 = 0.97 \text{ and } F = 72.2) \quad (2)$$

As observed with the analogues substituted at the C-4 position, the positive sign of the  $E_s$  parameter coefficient ( $0.38 \pm 0.05$ ) and the negative sign of the  $F$  parameter coefficient ( $-1.07 \pm 0.18$ ) suggest that the potency ( $\log K_i$ ) of MAO-B inhibition may be enhanced by substitution with sterically bulky C-3 functional groups that are electron-withdrawing (Fig. 2).

#### 2.4. Modeling studies

In an attempt to better understand the outcomes of the SAR study and to gain additional insight into the binding modes of the inhibitors, molecular docking of all the 1-methyl-3-phenylpyrroles (**5a–m**) within the active site of human MAO-B was performed. Among the crystallographic structures of MAO-B deposited in the Brookhaven Protein Data Bank, the structure with *trans,trans*-farnesol bound to the enzyme (2BK3.pdb)<sup>22</sup> was selected for the docking studies. The choice of this complex was based on the high resolution of the crystallographic structure and the observation that *trans,trans*-farnesol spans both the entrance and substrate cavities of the enzyme active site. As a result, the side chain of Ile-199, which acts as a ‘gate’ separating the two cavities, is rotated out of its normal conformation to allow for the fusion of the two cavities and the accommodation of larger structures.<sup>23</sup> In order to evaluate the accuracy of the docking procedure, the co-crystallized ligand was redocked within the active site using the LigandFit application of the molecular docking software, Discovery Studio 1.7.<sup>24</sup> The ligand to be docked was first constructed within DS Visualizer Pro and then prepared for the docking simulations using the Prepare Ligands application of Discovery Studio. Following the docking procedure, the docked ligand conformations were further refined using in situ ligand minimization with the Smart Minimizer algorithm. Even though *trans,trans*-farnesol has a relatively high degree of flexibility, the three best-ranked docking solutions obtained exhibited relatively small RMSD from the co-crystallized ligand ( $1.26 \pm 0.18$  Å). Within the best-ranked docking solutions, *trans,trans*-farnesol, however, also occupied reversed binding orientations which constituted approximately 40% of the 10 best docking solutions. Therefore, although the orientations of the best-ranked docking solutions obtained with LigandFit closely approximate that of the co-crystallized ligand, reversed binding poses can be expected to be among the docking solutions. Even with this limitation, LigandFit appears to be an effective molecular docking protocol for

examining the interactions of the inhibitors with the active site of MAO-B.

The best-ranked docking solutions obtained for all compounds examined (**5a–m**) indicate that the inhibitors traverse both the entrance and substrate cavities of the enzyme, with the pyrrolyl ring extending beyond the boundary between the entrance and substrate cavities while the phenyl ring binds within the substrate cavity. This orientation is probably favored in order to prevent unfavorable interactions between the N-CH<sub>3</sub> and the large polar regions of the substrate cavity and/or to maximize hydrophobic interactions of the N-CH<sub>3</sub> in the entrance cavity.<sup>25</sup> As shown by example with the most potent inhibitor of the series, **5e** (4-CF<sub>3</sub>), the phenyl ring is located in the substrate cavity (Fig. 3) while the pyrrolyl nucleus extends into the entrance cavity where the N-CH<sub>3</sub> is stabilized by the hydrophobic environment defined by Phe-103, Trp-119, Leu-164, Leu-167, Phe-168, Ile-316.<sup>25</sup> The best-ranked docking solutions of inhibitors **5b** (4-Cl), **5c** (4-Br), and **5f** (4-CH<sub>3</sub>) are virtually superimposed on the binding orientation of **5e**. Inhibitor **5a** (H) and **5d** (4-F) (Fig. 4) also adopt

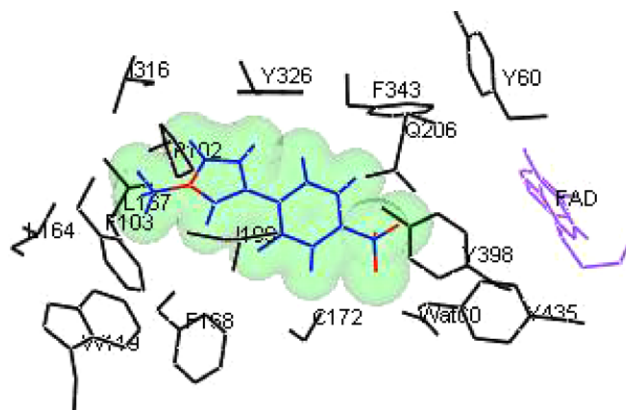


**Figure 3.** Schematic representation of the most stable complex between **5e** and MAO-B. The inhibitor is displayed in blue, the flavin in purple, and the residues of the enzymatic clefts in black.

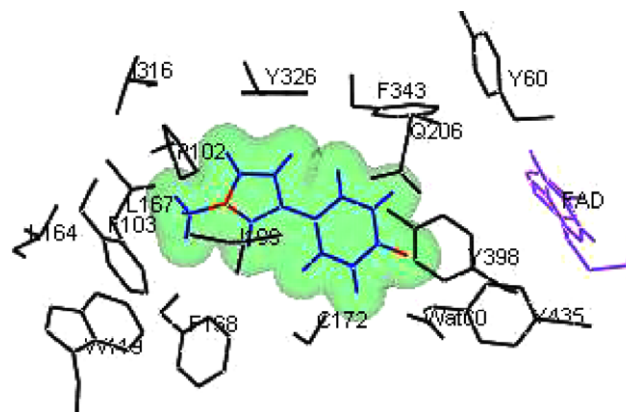


**Figure 4.** Schematic representation of the most stable complex between **5d** and MAO-B. The inhibitor is displayed in blue, the flavin in purple, and the residues of the enzymatic clefts in black.

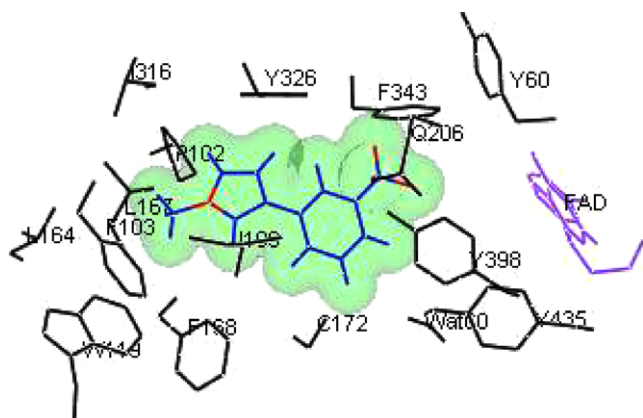


**Figure 5.** Schematic representation of the most stable complex between **5k** and MAO-B. The inhibitor is displayed in blue, the flavin in purple, and the residues of the enzymatic clefts in black.

similar binding modes, but the N-CH<sub>3</sub> protrudes to a lesser degree into the entrance cavity and hence is stabilized to a lesser extent (than **5e**) by the hydrophobic environment of the entrance cavity.

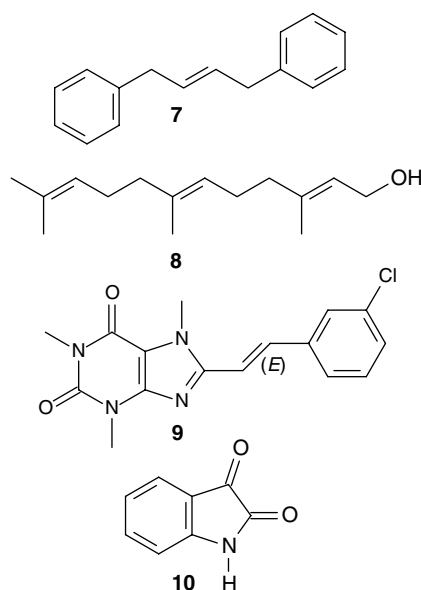
The 1-methyl-3-phenylpyrroles substituted at C-3 of the phenyl ring (**5h–m**) adopt similar binding orientations to the C-4 substituted analogues (Fig. 5). The principal difference is that the C-3 substituents are directed toward the small hydrophobic region defined by the apolar residues, Tyr-60, Phe-343, and Tyr-398, while the C-4 substituents are directed in the general direction of the aromatic cage defined by Tyr-398 and Tyr-435.<sup>25</sup> This binding mode presumably maximizes favorable hydrophobic contacts between the C-3 substituent and the enzyme while minimizing unfavorable interactions with the polar environment of the substrate cavity. As expected, the reverse binding modes are also represented among the 10 best-ranked docking solutions of the inhibitors examined, with a frequency of approximately 30–40%. The best solutions were, however, always orientated with the pyrrolyl ring directed toward the entrance cavity.

### 3. Discussion

This investigation shows that substitution of 1-methyl-3-phenylpyrroles on the phenyl ring has a considerable effect on the potency of MAO-B inhibition displayed by these compounds. For example, substitution at C-4 with a trifluoromethyl functional group (**5e**) increases the inhibition potency by approximately 90-fold compared to the unsubstituted 1-methyl-3-phenylpyrrole (**5a**). The SAR analysis indicates that the inhibition activities correlate with the Taft steric parameter and the Swain–Lupton constant of the substituents at both C-4 and C-3 of the phenyl ring. Inhibitor binding to the enzyme is favored by an increase in both the steric bulk and the electronegativity of the *para* and *meta* substituents.

Interestingly 1-methyl-3-phenylpyrroles do not seem to be inhibitors of beef liver MAO-B since the most potent inhibitor examined here, **5e**, does not inhibit beef liver

MAO-B, even at a concentration of 200 μM which is well above its *K<sub>i</sub>* value (1.30 μM) for the inhibition of baboon liver MAO-B. Beef liver MAO-B was also not inhibited by any of the other pyrrolyl derivatives examined here. Other compounds (Scheme 4), 1,4-diphenyl-2-butene (**7**),<sup>23</sup> *trans,trans*-farnesol (**8**)<sup>26</sup>, and (*E*)-8-(3-chlorostyryl)caffeine (**9**),<sup>27</sup> have also been reported to inhibit baboon liver and recombinant human MAO-B competitively while having no effect on beef MAO-B. The crystal structures of human recombinant MAO-B in complex with **7** and **8** have shown that these reversible inhibitors exhibit a dual binding mode that involves traversing both the entrance and substrate cavities of the enzyme.<sup>23</sup> The ‘gate’ separating the two cavities is the side chain of Ile-199 which is rotated out of its normal conformation to allow for the fusion of the two cavities in order to accommodate these larger inhibitors.<sup>23</sup> In contrast to **7** and **8**, the small molecule inhibitor isatin (**10**) has been shown to inhibit competitively all known MAO-B isoforms, including the beef isoform, with similar potencies.<sup>22</sup> Crystal structures of human recombinant MAO-B in complex with isatin<sup>23</sup> have shown that isatin binds within the substrate cavity, leaving the entrance cavity unoccupied. In this instance the side chain of Ile-199 exhibits the normal or ‘closed’ rotamer conformation. Ile-199 is conserved in all known MAO-B sequences with the exception of beef MAO-B where it is replaced with Phe. The increased size of the Phe aromatic ring relative to Ile is suggested to prevent its occupation of the ‘open’ rotamer conformation.<sup>22</sup> The only available space for the aromatic ring to occupy is in the entrance cavity of the enzyme which prevents the binding of inhibitors that must traverse both cavities.<sup>22</sup> The observation that **5a–m** does not inhibit beef liver MAO-B suggests that binding of 1-methyl-3-phenylpyrroles to the active site of MAO-B is dependent upon the rotation of Ile-199 out of its normal conformation. This implies that 1-methyl-3-phenylpyrroles also exhibit a



**Scheme 4.** The structures of the reversible MAO-B inhibitors 1,4-diphenyl-2-butene (**7**), *trans,trans*-farnesol (**8**), (*E*)-8-(3-chlorostyryl)caffeine (**9**), and isatin (**10**).

dual binding mode that involves interactions with both the entrance and substrate cavities.

While the exact binding orientation of 1-methyl-3-phenylpyrroles in the active site of MAO-B is unknown, molecular docking studies support the argument that the inhibitors occupy both cavities. The most stable protein-inhibitor models generated indicate that the inhibitors may bind to MAO-B with the pyrrolyl moiety protruding into the entrance cavity while the phenyl ring is located within the substrate cavity (Figs. 3–5). For this binding mode to be possible, the side chain of Ile-199 must be rotated into the ‘open’ conformation. The pyrrolyl N–CH<sub>3</sub> appears to be stabilized by the hydrophobic environment of the entrance cavity and as a result, the structural features of the inhibitor that allow for a higher degree of projection of the N–CH<sub>3</sub> into the entrance cavity, may enhance inhibition potency. One such feature may be enhanced steric bulk of the phenyl substituents. In accordance with this idea, the SAR analysis showed that the inhibition activity correlated with the Taft steric parameter of the substituents at both C-4 and C-3.

The apparent contribution of the Swain–Lupton constant (*F*) of the phenyl substituents toward the correlations of the inhibition potency with *E<sub>s</sub>* and *F* (Eqs. 1 and 2) is not well understood. Electron-withdrawing substituents at C-3 and C-4 enhance MAO-B inhibition potency of 1-methyl-3-phenylpyrroles. This is also apparent from the moderate correlations of 0.60 (Table 2) and 0.71 (Table 3) recorded between the log *K<sub>i</sub>* values and the Hammett electronic parameters (*σ<sub>p</sub>* or *σ<sub>m</sub>*). A possible explanation may be that electron-withdrawing functionalities promote planarity between the phenyl and pyrrolyl rings. The literature supports the idea that planar, heterocyclic compounds frequently act as competitive inhibitors of MAO-B.<sup>28,29</sup> The shift to longer wavelengths of maximal light absorption (*λ<sub>max</sub>*) upon substitution of the phenyl ring by electron-withdrawing functional groups (CF<sub>3</sub>, Br, and Cl) may support this hypothesis. As shown in Table 4, the more potent inhibitors examined in this study (CF<sub>3</sub>, Br, and Cl) exhibited *λ<sub>max</sub>* values of 276–286 nm while the relatively less potent inhibitors (H, F, CH<sub>3</sub>, and OCH<sub>3</sub>) were found to have *λ<sub>max</sub>* values of 264–272 nm.

**Table 4.** The wavelengths of maximal light absorption (*λ<sub>max</sub>*) of 1-methyl-3-phenylpyrrolyl derivatives (**5a–m**)

Compound	<i>λ<sub>max</sub></i> (nm) <sup>a</sup>	<i>ε</i> (M <sup>-1</sup> )
<b>5a</b>	268	13,880
<b>5b</b>	276	18,260
<b>5c</b>	279	18,660
<b>5d</b>	264	12,360
<b>5e</b>	286	15,060
<b>5f</b>	269	15,460
<b>5g</b>	268	17,280
<b>5h</b>	276	13,700
<b>5i</b>	277	13,880
<b>5j</b>	272	13,420
<b>5k</b>	277	13,640
<b>5l</b>	270	13,660
<b>5m</b>	269	12,220

The extinction coefficients (*ε*) at these wavelengths are also listed.

<sup>a</sup>All UV/Vis spectral measurements were conducted in isopropanol.

In conclusion, even though none of the 1-methyl-3-phenylpyrroles examined here were found to be exceptionally potent inhibitors of MAO-B, this study reveals the general structural features that are important for MAO-B inhibition as well as the modifications that can be made in order to enhance inhibition potency. Features important for inhibition are coplanarity of the aromatic rings and bulky electronegative substituents at the *para* and *meta* positions of the phenyl ring. Structural modifications that may enhance inhibition potency are the enhancement of the distance between the pyrrolyl and phenyl rings (e.g., with an ethylene linker) and the inclusion of additional lipophilic substituents on the pyrrolyl ring (e.g., CH<sub>3</sub> at position 2 and/or 5). Both these modifications will have the effect of promoting hydrophobic burial of the pyrrolyl ring in the entrance cavity of MAO-B.

## 4. Experimental

**Caution.** MMTP is a structural analogue of the nigrostriatal neurotoxin 1-methyl-4-phenyl-1,2,3,6-tetrahydropyridine (MPTP) and should be handled using disposable gloves and protective eyewear. Procedures for the safe handling of MPTP have been described previously.<sup>30</sup>

### 4.1. Chemicals and instrumentation

All starting materials not described elsewhere were obtained from Sigma–Aldrich and were used without purification. The oxalate salt of MMTP was prepared as described previously.<sup>7</sup> Petroleum ether used in this study was of a distillation range of 40–60 °C. Proton and carbon NMR spectra were recorded on a Varian Gemini 300 spectrometer. Proton (<sup>1</sup>H) spectra were recorded in CDCl<sub>3</sub> and *d*<sub>6</sub>-DMSO at a frequency of 300 MHz and carbon (<sup>13</sup>C) spectra at 75 MHz. Chemical shifts are reported in parts per million (*δ*) downfield from the signal of tetramethylsilane added to the deuterated solvent. Spin multiplicities are given as s (singlet), d (doublet), t (triplet), q (quartet), dd (doublet of doublets) or m (multiplet) and the coupling constants (*J*) are given in hertz (Hz). Direct insertion electron impact ionization (EIMS), high resolution (HRMS), and fast atom bombardment (FAB-MS) mass spectra were obtained on a VG 7070E mass spectrometer. Melting points (mp) were determined on a Gallenkamp melting point apparatus and are uncorrected. UV–Vis spectra were recorded on a Milton-Roy Spectronic 1201 spectrophotometer. Thin layer chromatography (TLC) was carried out with neutral aluminium oxide 60 (Merck) containing UV<sub>254</sub> fluorescent indicator.

### 4.2. Synthesis of 2-aryl-3-(dimethylamino)allylidene (dimethyl)ammonium perchlorates (**6a–m**)

Synthetic intermediates **6a–m** were prepared in relatively high yields from the corresponding phenylacetic acid, DMF, and phosphoryl chloride according the method described in the literature.<sup>14</sup> The melting points of the compounds reported previously were as follows: **6a** mp

203–205 °C (from ethanol), lit. mp 193–194 °C<sup>14</sup>; **6b** mp 149–151 °C (from ethanol), lit. mp 142–144 °C<sup>14</sup>; **6c** mp 162–164 °C (from ethanol), lit. mp 152–154 °C<sup>14</sup>; **6f** mp 165–166 °C (from ethanol), lit. mp 150–152 °C<sup>31</sup>; **6g** mp 134–136 °C (from ethanol), lit. mp 130–131 °C<sup>14</sup>; **6h** mp 186–188 °C (from ethanol), lit. mp 180 °C<sup>32</sup>; **6k** mp 114–116 °C (from ethanol), lit. mp 141.5–143 °C<sup>33</sup>; **6l** mp 160–162 °C (from ethanol), lit. mp 164–166 °C.<sup>33</sup> The characterizations of compounds that are previously unreported are summarized below.

*2-(4-Fluorophenyl)-3-(dimethylamino)allylidene(dimethyl) ammonium perchlorate (6d)* was synthesized from 4-fluorophenylacetic acid in a yield of 67.8%: mp 144–146 °C (from ethanol); <sup>1</sup>H NMR (*d*<sub>6</sub>-DMSO) δ 2.44 (s, 6H), 3.24 (s, 6H), 7.23–7.37 (m, 4H), 7.69 (s, 2H); <sup>13</sup>C NMR (*d*<sub>6</sub>-DMSO) δ 39.30, 48.53, 103.82, 115.25 (d), 128.73 (d), 134.12 (d), 160.47, 163.02, 163.73; FAB-MS *m/z* 221 (M<sup>+</sup>).

*2-(4-Trifluoromethylphenyl)-3-(dimethylamino)allylidene(dimethyl) ammonium perchlorate (6e)* was synthesized from 4-(trifluoromethyl)phenylacetic acid in a yield of 72.9%: mp 151–154 °C (from ethanol); <sup>1</sup>H NMR (*d*<sub>6</sub>-DMSO) δ 2.42 (s, 6H), 3.26 (s, 6H), 7.56 (d, 2H, *J* = 7.8 Hz), 7.75–7.79 (m, 4H); <sup>13</sup>C NMR (*d*<sub>6</sub>-DMSO) δ 48.59, 103.24, 122.16, 124.96 (q), 125.77, 128.99 (q), 132.95, 137.45, 162.83; FAB-MS *m/z* 271 (M<sup>+</sup>).

*2-(3-Bromophenyl)-3-(dimethylamino)allylidene(dimethyl) ammonium perchlorate (6i)* was synthesized from 3-bromophenylacetic acid in a yield of 80.4%: mp 177–178 °C (from ethanol); <sup>1</sup>H NMR (*d*<sub>6</sub>-DMSO) δ 2.46 (s, 6H), 3.24 (s, 6H), 7.31–7.41 (m, 2H), 7.57 (t, 1H, *J* = 1.6 Hz), 7.62–7.65 (m, 1H), 7.69 (s, 2H); <sup>13</sup>C NMR (*d*<sub>6</sub>-DMSO) δ 48.55, 103.32, 121.53, 130.21, 131.24, 131.57, 134.44, 135.15, 162.75; FAB-MS *m/z* 281, 283 (M<sup>+</sup>).

*2-(3-Fluorophenyl)-3-(dimethylamino)allylidene(dimethyl) ammonium perchlorate (6j)* was synthesized from 3-fluorophenylacetic acid in a yield of 78.1%: mp 158–161 °C (from ethanol); <sup>1</sup>H NMR (*d*<sub>6</sub>-DMSO) δ 2.46 (s, 6H), 3.24 (s, 6H), 7.14–7.22 (m, 2H), 7.24–7.31 (m, 1H), 7.43–7.51 (m, 1H), 7.70 (s, 2H); <sup>13</sup>C NMR (*d*<sub>6</sub>-DMSO) δ 39.33, 48.54, 103.53, 115.65 (d), 118.97 (d), 128.56 (d), 130.25 (d), 134.98 (d), 159.90, 162.76, 163.17; FAB-MS *m/z* 222 (MH<sup>+</sup>).

*2-(3-Methoxyphenyl)-3-(dimethylamino)allylidene(dimethyl) ammonium perchlorate (6m)* was synthesized from 3-methoxyphenylacetic acid in a yield of 75.8%: mp 148–150 °C (from ethanol); <sup>1</sup>H NMR (*d*<sub>6</sub>-DMSO) δ 2.47 (s, 6H), 3.23 (s, 6H), 3.77 (s, 3H), 6.85–6.87 (m, 2H), 6.97–7.01 (m, 1H), 7.31–7.36 (m, 1H), 7.67 (s, 2H); <sup>13</sup>C NMR (*d*<sub>6</sub>-DMSO) δ 48.46, 55.16, 104.86, 114.47, 117.40, 124.48, 129.41, 133.79, 158.94, 162.73; FAB-MS *m/z* 233 (M<sup>+</sup>).

#### 4.3. Synthesis of 1-methyl-3-phenylpyrroles (5a–m)

The 1-methyl-3-phenylpyrrolyl derivatives (**5a–m**) were synthesized from the corresponding 2-aryl-3-(dimethylamino)allylidene(dimethyl)ammonium perchlorates

(**6a–m**) according to a modification of the method described in the literature.<sup>13</sup> Sodium wire (143 mmol) was reacted with methanol (48 mL) and the resulting solution was added under an atmosphere of argon to a solution of **6** (64.8 mmol) in 262 mL dry pyridine (distilled over CaH<sub>2</sub> and stored over 4 Å molecular sieves). The reaction was heated under reflux for 24 h. The pyridine was removed via vacuum distillation to obtain a yellow pasty residue to which 100 mL distilled water was added. The resulting suspension was extracted with ethylacetate (3 × 100 mL) and the combined organic phases were dried over anhydrous magnesium sulfate (10 g). After the solvent was removed under reduced pressure an oily residue was obtained. The crude product was dissolved in a minimal amount of ethylacetate and purified on a short column (35 × 80 mm) by neutral aluminium oxide chromatography (Fluka 507C) with 100% petroleum ether (**5a–b, f, and k–l**) or petroleum ether/ethylacetate, 90:10 (**5g and m**), as mobile phase. The fractions containing the product were in most cases recrystallized from an appropriate solvent as cited below. For the synthesis of **5c–e** and **5h–j**, the following modifications were made: following the addition of the 100 mL distilled water to the yellow pasty residue obtained from the vacuum distillation of the pyridine solvent, a suspension was obtained which was stirred for 60 min at room temperature and filtered. A yellow solid residue was obtained which was recrystallized from an appropriate solvent as cited below. All reactions were monitored using neutral aluminium oxide TLC (mobile phase of 100% petroleum ether). The TLC plates were visualized with UV light (254 nm) or by staining with iodine. The melting points of compounds reported previously were as follows: **5a** mp 44–46 °C (from petroleum ether), lit. mp 46–47 °C<sup>13</sup>; **5b** mp 112–114 °C (from methanol), lit. mp 117.5–119.5 °C<sup>13</sup>; **5c** mp 129–130 °C (from methanol), lit. mp 132–133 °C<sup>13</sup>; **5f** mp 49–51 °C (from methanol), lit. mp 55–56 °C<sup>34</sup>; **5g** mp 120–122 °C (from methanol), lit. mp 126–128 °C<sup>13</sup>; **5j** mp 73–75 °C (from methanol), lit. mp 94–96 °C.<sup>13</sup> The characterizations of compounds that were previously unreported are summarized below.

*1-Methyl-3-(4-fluorophenyl)pyrrole (5d)* was synthesized from **6d** in a yield of 31.5%: mp 98–100 °C (from methanol); <sup>1</sup>H NMR (CDCl<sub>3</sub>) δ 3.67 (s, 3H), 6.37 (dd, 1H, *J* = 1.8, 2.7 Hz), 6.61 (t, 1H, *J* = 2.5 Hz), 6.83 (t, 1H, *J* = 2.1 Hz), 7.00 (m, 2H), 7.42 (m, 2H); <sup>13</sup>C NMR (CDCl<sub>3</sub>) δ 36.27, 106.26, 115.29 (d), 118.26, 122.78, 124.17, 126.32 (d), 132.13, 132.17; EIMS *m/z* 175 (M<sup>+</sup>); HRMS calcd 175.0797, found 175.0811.

*1-Methyl-3-(4-trifluoromethylphenyl)pyrrole (5e)* was synthesized from **6e** in a yield of 41.1%: mp 161–162 °C (from methanol); <sup>1</sup>H NMR (CDCl<sub>3</sub>) δ 3.68 (s, 3H), 6.45 (dd, 1H, *J* = 1.8, 2.8 Hz), 6.34 (t, 1H, *J* = 2.5 Hz), 6.96 (t, 1H, *J* = 2.0 Hz), 7.00 (s, 4H); <sup>13</sup>C NMR (CDCl<sub>3</sub>) δ 36.37, 106.53, 119.39, 123.19, 123.63, 124.75, 125.52 (q), 139.53; EIMS *m/z* 225 (M<sup>+</sup>); HRMS calcd 225.0765, found 225.0757.

*1-Methyl-3-(3-chlorophenyl)pyrrole (5h)* was synthesized from **6h** in a yield of 33.6%: mp 77–80 °C (from

methanol);  $^1\text{H}$  NMR ( $\text{CDCl}_3$ )  $\delta$  3.66 (s, 3H), 6.41 (t, 1H,  $J = 2.3$  Hz), 6.62 (t, 1H,  $J = 2.5$  Hz), 6.90 (t, 1H,  $J = 2.0$  Hz), 7.09–7.13 (m, 1H), 7.20–7.26 (m, 1H), 7.34–7.38 (m, 1H), 7.48 (t, 1H,  $J = 1.9$  Hz);  $^{13}\text{C}$  NMR ( $\text{CDCl}_3$ )  $\delta$  36.30, 106.33, 118.93, 122.95, 123.66, 124.87, 125.05, 129.74, 134.39, 137.87; EIMS  $m/z$  191 ( $\text{M}^+$ ); HRMS calcd 191.0502, found 191.0490.

*1-Methyl-3-(3-bromophenyl)pyrrole (5i)* was synthesized from **6i** in a yield of 36.9%: mp 82–84 °C (from methanol);  $^1\text{H}$  NMR ( $\text{CDCl}_3$ )  $\delta$  3.65 (s, 3H), 6.39 (dd, 1H,  $J = 1.8, 2.7$  Hz), 6.60 (t, 1H,  $J = 2.5$  Hz), 6.87 (t, 1H,  $J = 2.0$  Hz), 7.15 (m, 1H), 7.22–7.26 (m, 1H), 7.36–7.40 (m, 1H), 7.61 (t, 1H,  $J = 1.9$  Hz);  $^{13}\text{C}$  NMR ( $\text{CDCl}_3$ )  $\delta$  36.32, 106.34, 118.93, 122.75, 122.96, 123.40, 123.55, 127.80, 127.96, 130.03, 138.18; EIMS  $m/z$  235, 237 ( $\text{M}^+$ ); HRMS calcd 234.9997, found 235.0003.

*1-Methyl-3-(3-trifluoromethylphenyl)pyrrole (5k)* was synthesized from **6k** in a yield of 51.9%: mp 41–44 °C;  $^1\text{H}$  NMR ( $\text{CDCl}_3$ )  $\delta$  3.68 (s, 3H), 6.45 (dd, 1H,  $J = 1.8, 2.7$  Hz), 6.64 (t, 1H,  $J = 2.4$  Hz), 6.95 (t, 1H,  $J = 2.0$  Hz), 7.39 (m, 2H), 7.62–7.66 (m, 1H), 7.71 (m, 1H);  $^{13}\text{C}$  NMR ( $\text{CDCl}_3$ )  $\delta$  36.34, 106.37, 119.04, 121.49 (q), 121.69 (q), 122.61, 123.12, 123.69, 126.22, 127.99, 128.92, 136.79; EIMS  $m/z$  225 ( $\text{M}^+$ ); HRMS calcd 225.0765, found 225.0764.

*1-Methyl-3-(3-methylphenyl)pyrrole (5l)* was synthesized from **6l** in a yield of 72.7%: mp 39–42 °C;  $^1\text{H}$  NMR ( $\text{CDCl}_3$ )  $\delta$  2.38 (s, 3H), 3.68 (s, 3H), 6.45 (dd, 1H,  $J = 1.8, 2.7$  Hz), 6.62 (t, 1H,  $J = 2.5$  Hz), 6.90 (t, 1H,  $J = 2.0$  Hz), 6.97–7.01 (m, 1H), 7.20–7.25 (m, 1H), 7.30–7.35 (m, 2H);  $^{13}\text{C}$  NMR ( $\text{CDCl}_3$ )  $\delta$  21.50, 36.24, 106.35, 118.51, 122.12, 122.58, 125.11, 125.79, 126.02, 128.43, 135.88, 137.96; EIMS  $m/z$  171 ( $\text{M}^+$ ); HRMS calcd 171.1048, found 171.1049.

*1-Methyl-3-(3-methoxyphenyl)pyrrole (5m)* was synthesized from **6m** in a yield of 62.0%: mp 67–70 °C;  $^1\text{H}$  NMR ( $\text{CDCl}_3$ )  $\delta$  3.67 (s, 3H), 3.84 (s, 3H), 6.45 (dd, 1H,  $J = 1.8, 2.7$  Hz), 6.62 (t, 1H,  $J = 2.5$  Hz), 6.71–6.75 (m, 1H), 6.91 (t, 1H,  $J = 2.0$  Hz), 7.06 (dd, 1H,  $J = 1.6, 2.5$  Hz), 7.10–7.13 (m, 1H), 7.23–7.08 (m, 1H);  $^{13}\text{C}$  NMR ( $\text{CDCl}_3$ )  $\delta$  36.23, 55.12, 106.40, 110.59, 110.73, 117.66, 118.71, 122.63, 128.86, 129.46, 137.42, 158.89; EIMS  $m/z$  187 ( $\text{M}^+$ ); HRMS calcd 187.0997, found 187.1004.

#### 4.4. MAO-B inhibition studies

Mitochondria were isolated from baboon and beef liver tissue as described by Salach and Weyler<sup>35</sup> and stored at –70 °C in 300  $\mu\text{L}$  aliquots. Following addition of an equal volume of sodium phosphate buffer (100 mM, pH 7.4) containing glycerol (50%, w/v) to the aliquots, the protein concentration was determined by the method of Bradford using bovine serum albumin as reference standard.<sup>36</sup> Since the mitochondrial fraction obtained from baboon and beef liver tissue is reported to be devoid of MAO-A activity,<sup>15</sup> inactivation of this isoform was unnecessary. The MAO-A and -B mixed substrate MMTP ( $K_m = 60.9 \mu\text{M}$  for baboon liver MAO-B)<sup>15</sup>

served as substrate for the inhibition studies. Incubations were carried out in sodium phosphate buffer (100 mM, pH 7.4) and contained MMTP (30–120  $\mu\text{M}$ ), the mitochondrial isolate (0.15 mg protein/mL), and various concentrations of the test inhibitors. The final volume of the incubations was 500  $\mu\text{L}$ . The stock solutions of the inhibitors were prepared in DMSO and were added to the incubation mixtures to yield a final DMSO concentration of 4% (v/v). DMSO concentrations higher than 4% are reported to inhibit MAO-B.<sup>29</sup> Following incubation at 37 °C for 15 min, the enzyme reactions were terminated by the addition of 10  $\mu\text{L}$  perchloric acid (70%) and the samples were centrifuged at 16,000g for 10 min. The MAO-B catalyzed production of MMDP<sup>+</sup> is reported to be linear for the first 15 min of incubation under these conditions.<sup>15</sup> The supernatant fractions were removed and the concentrations of the MAO-B generated product, MMDP<sup>+</sup>, were measured spectrophotometrically at a wavelength of 420 nm ( $\epsilon = 25,000 \text{ M}^{-1}$ ).<sup>15</sup> The initial rates of oxidation at four different substrate concentrations (30–120  $\mu\text{M}$ ) in the absence and presence of three different concentrations of the inhibitors were calculated and Lineweaver–Burk plots were constructed. The slopes of the Lineweaver–Burk plots were plotted versus the inhibitor concentration and the  $K_i$  value was determined from the  $x$ -axis intercept (intercept =  $-K_i$ ). Linear regression analysis was performed using the SigmaPlot software package (Systat Software Inc.). Each  $K_i$  value reported here is representative of a single determination where the correlation coefficient ( $R^2$  value) of the replot of the slopes versus the inhibitor concentrations was at least 0.98.

#### 4.5. Time-dependent inhibition studies

In order to determine whether the test inhibitor **5e** acts as a time-dependent inactivator or reversible inhibitor of MAO-B, baboon liver mitochondrial fractions (0.3 mg of protein/mL) were preincubated with **5e** (5.20  $\mu\text{M}$ ) for periods of 0, 15, 30, and 60 min at 37 °C.<sup>15</sup> The solvent for this incubation was 100 mM sodium phosphate buffer (pH 7.4). The MAO-A/B mixed substrate, MMTP, at final concentration of 90  $\mu\text{M}$ , was then incubated at 37 °C for 15 min with 0.15 mg protein/mL of the preincubated mitochondria. The final volumes of these incubations were 500  $\mu\text{L}$  and the final concentration of the test inhibitor 2.60  $\mu\text{M}$ . Following termination of the reactions by the addition of 10  $\mu\text{L}$  of perchloric acid (70%), the concentrations of MMDP<sup>+</sup> were measured as outlined above. These experiments were carried out in triplicate.

#### 4.6. SAR studies

The values of the substituent descriptors  $\sigma_p$ ,  $\sigma_m$ ,  $F$ ,  $\pi$ , and  $E_s$  were obtained from Hansch and Leo<sup>19</sup> while those for the Van der Waals volume ( $V_w$ ) were obtained from compilations by Van de Waterbeemb and Testa.<sup>20</sup> Linear regression analysis of the  $\log K_i$  values as a function of the substituent descriptor values was carried out with Statistica software package (StatSoft Inc.). In order to estimate the significance of the regression equations, the  $F$  statistic was employed. An  $F$  value higher than

the critical  $F$  value was judged to be significant. The critical  $F$  value ( $F_{\max}$ ) for 95% significance for models constructed from seven  $\log K_i$  values (Tables 2 and 3) and which contain one parameter (out of a possible five:  $V_w$ ,  $E_s$ ,  $\pi$ ,  $\sigma_{p/m}$ , and  $F$ ) was calculated to be 25.32, while the  $F_{\max}$  value for models containing two parameters was calculated to be 30.18.<sup>21</sup>

#### 4.7. Molecular docking studies

All the computational studies were carried out in the Windows-based Discovery Studio 1.7 modeling and simulation environment.<sup>24</sup> The ligands to be docked were constructed within DS Visualizer Pro and then prepared for the docking simulations using the Prepare Ligands application of Discovery Studio. The crystallographic structure of *trans,trans*-farnesol in complex with human MAO-B (2BK3.pdb)<sup>22</sup> was retrieved from the Brookhaven Protein Data Bank ([www.rcsb.org/pdb](http://www.rcsb.org/pdb)) and the co-crystallized inhibitor was manually deleted. Following typing of the receptor model with the CHARMM forcefield, the binding site was identified by the LigandFit flood-filling algorithm. Automated docking was then carried out with the LigandFit application of Discovery Studio. This docking protocol employed total ligand flexibility whereby the final ligand conformations were determined by the Monte Carlo conformation search method set to a variable number of trial runs. The docked ligands were further refined using in situ ligand minimization with the Smart Minimizer algorithm. All the application modules within Discovery Studio were set to their default values and 10 docking solutions were allowed for each ligand.

#### Acknowledgments

The NMR and MS spectra were recorded by André Joubert, Johan Jordaan, and Louis Fourie of the SASOL Centre for Chemistry, North-West University. This work was supported by grants from the National Research Foundation and the Medical Research Council, South Africa.

#### References and notes

- Chiba, K.; Trevor, A. J.; Castagnoli, N., Jr. *Biochem. Biophys. Res. Commun.* **1984**, *120*, 574.
- Heikkila, R. E.; Manzino, L.; Cabbat, F. S.; Duvoisin, R. C. *Nature* **1984**, *311*, 467.
- Nicklas, W. J.; Vyas, I.; Heikkila, R. E. *Life Sci.* **1985**, *36*, 2503.
- Ramsay, R. R.; Krueger, M. J.; Youngster, S. K.; Gluck, M. R.; Casida, J. E.; Singer, T. P. *J. Neurochem.* **1991**, *56*, 1184.
- Kalgutkar, A. S.; Castagnoli, N., Jr. *J. Med. Chem.* **1992**, *35*, 4165.
- Rimoldi, J. M.; Puppali, S. G.; Isin, E.; Bissel, P.; Khalil, A.; Castagnoli, N., Jr. *Bioorg. Med. Chem.* **2005**, *13*, 5808.
- Bissel, P.; Bigley, M. C.; Castagnoli, K.; Castagnoli, N., Jr. *Bioorg. Med. Chem.* **2002**, *10*, 3031.
- Wang, Y. X.; Mabic, S.; Castagnoli, N., Jr. *Bioorg. Med. Chem.* **1998**, *6*, 143.
- Williams, C. H.; Lawson, J. *Biochem. J.* **1998**, *336*, 63.
- Williams, C. H.; Lawson, J. *Neurobiology (Bp)* **1999**, *7*, 225.
- Youdim, M. B. H.; Bakhle, Y. S. *Br. J. Pharmacol.* **2006**, *147*, S287.
- Youdim, M. B. H.; Edmondson, D.; Tipton, K. F. *Nat. Rev. Neurosci.* **2006**, *7*, 295.
- Gallagher, P. T.; Palmer, J. L.; Morgan, S. E. *J. Chem. Soc., Perkin Trans. 1* **1990**, *11*, 3212.
- Jutz, C.; Kirchlechner, R.; Siedel, H. J. *Chem. Ber.* **1969**, *102*, 2301.
- Inoue, H.; Castagnoli, K.; Van der Schyf, C. J.; Mabic, S.; Igarashi, K.; Castagnoli, N., Jr. *J. Pharmacol. Exp. Ther.* **1999**, *291*, 856.
- Vlok, N.; Malan, S. F.; Castagnoli, N., Jr.; Bergh, J. J.; Petzer, J. P. *Bioorg. Med. Chem.* **2006**, *14*, 3512.
- Petzer, J. P.; Steyn, S.; Castagnoli, K. P.; Chen, J. F.; Schwarzschild, M. A.; Van der Schyf, C. J.; Castagnoli, N., Jr. *Bioorg. Med. Chem.* **2003**, *11*, 1299.
- Khalil, A. A.; Steyn, S.; Castagnoli, N., Jr. *Chem. Res. Toxicol.* **2000**, *13*, 31.
- Hansch, C.; Leo, A. *Exploring QSAR. Fundamentals and Applications in Chemistry and Biology*; American Chemical Society: Washington, DC, 1995, pp 1–124.
- Van de Waterbeemb, H.; Testa, B. In *Advances in Drug Research*; Testa, B., Ed.; Academic Press: London, 1987; pp 85–225.
- Livingstone, D. J.; Salt, D. W. *J. Med. Chem.* **2005**, *48*, 661.
- Hubálek, F.; Binda, C.; Khalil, A.; Li, M.; Mattevi, A.; Castagnoli, N., Jr.; Edmondson, D. E. *J. Biol. Chem.* **2005**, *280*, 15761.
- Binda, C.; Li, M.; Hubálek, F.; Restelli, N.; Edmondson, D. E.; Mattevi, A. *Proc. Natl. Acad. Sci. U.S.A.* **2003**, *100*, 9750.
- Accelrys Discovery Studio 1.7, Accelrys Software Inc., San Diego, CA, USA, <http://www.accelrys.com>.
- Novaroli, L.; Daina, A.; Favre, E.; Bravo, J.; Carotti, A.; Leonetti, F.; Catto, M.; Carrupt, P. A.; Reist, M. *J. Med. Chem.* **2006**, *49*, 6264.
- Khalil, A. A.; Davies, B.; Castagnoli, N., Jr. *Bioorg. Med. Chem.* **2006**, *14*, 3392.
- Chen, J. F.; Xu, K.; Petzer, J. P.; Staal, R.; Xu, Y. H.; Beilstein, M.; Sonsalla, P. K.; Castagnoli, K.; Castagnoli, N., Jr.; Schwarzschild, M. A. *J. Neurosci.* **2001**, *21*, RC143.
- Castagnoli, K.; Palmer, S.; Anderson, A.; Bueters, T.; Castagnoli, N., Jr. *Chem. Res. Toxicol.* **1997**, *10*, 364.
- Gnerre, C.; Catto, M.; Leonetti, F.; Weber, P.; Carrupt, P. -A.; Altomare, C.; Carotti, A.; Testa, B. *J. Med. Chem.* **2000**, *43*, 4747.
- Pitts, S. M.; Markey, S. P.; Murphy, D. L.; Weisz, A. In *MPTP: A Neurotoxin Producing a Parkinsonian Syndrome*; Markey, S. P., Castagnoli, N., Jr., Trevor, A. J., Kopin, I. J., Eds.; Academic Press: New York, 1986; pp 703–716.
- Lloyd, D.; Tucker, K. S.; Marshall, D. R. *J. Chem. Soc., Perkin Trans. 1* **1981**, 726.
- Allen, D. W.; Buckland, D. J.; Hutley, B. G. *Z. Naturforsch., B: Anorg. Chem., Org. Chem.* **1980**, *35*, 463.
- Church, R.; Trust, R.; Albright, D.; Powell, D. W. *J. Org. Chem.* **1995**, *60*, 3750.
- Hauptmann, S.; Weisflog, J. *J. Prakt. Chem.* **1972**, *314*, 353.
- Salach, J. I.; Weyler, W. *Methods Enzymol.* **1987**, *142*, 627.
- Bradford, M. M. *Anal. Biochem.* **1976**, *72*, 248.